CARBONATE CEMENTATION IN A SEQUENCE-STRATIGRAPHIC FRAMEWORK: UPPER CRETACEOUS SANDSTONES, BOOK CLIFFS, UTAH–COLORADO

KEVIN G. TAYLOR[1]*, ROB L. GAWTHORPE[1], CHARLES D. CURTIS[1], JIM D. MARSHALL[2], AND DAVID N. AWWILLER[3]
[1] *Department of Earth Sciences, University of Manchester, Oxford Road, Manchester M13 9PL, U.K.*
[2] *Department of Earth Sciences, University of Liverpool, PO Box 147, Liverpool L69 3BX, U.K.*
[3] *Exxon Production Research Co., Houston, Texas, U.S.A.*

ABSTRACT: **Three macroscopic diagenetic features can be recognized in the sandstones of the Upper Cretaceous Desert Member of the Blackhawk Formation and Castlegate Sandstone of the Mesaverde Group exposed in the Book Cliffs, Utah, each of which have distinctive form, geometry, and stratigraphic distribution. Diagenetic alterations are: (1) leached zones (''whitecaps''), up to 10 m thick, beneath coal beds; (2) large (up to 8 m) concretionary carbonate-cemented bodies in amalgamated shoreface and thin fluvial sandstones; and (3) thin (up to 2 m), laterally extensive carbonate-cemented horizons beneath major marine flooding surfaces. Each feature has distinct petrographic and geochemical signatures, and formed through discrete diagenetic processes. Large isolated carbonate-cemented bodies are composed of ferroan dolomite, most of which precipitated during early diagenesis. Field and petrographic data, coupled with stable-isotope data (early cements, $\delta^{13}C = -2.5$ to $+3.4$‰ VPDB; $\delta^{18}O = -7.8$ to -12.0‰ VPDB; $^{87}Sr/^{86}Sr = 0.7078$; later cements, $\delta^{13}C = -3.1$ to -5.7‰ VPDB; $\delta^{18}O = -12.0$ to -15.1‰ VPDB; $^{87}Sr/^{86}Sr = 0.7093$) suggest precipitation from meteoric fluids, input into sediments during times of relative sea-level fall. The source of carbonate for the dolomite cement was dissolution of detrital dolomite from beneath coals by organic acids and subsequent mobilization by meteoric fluids. Carbonate precipitation in laterally extensive cement horizons appears to have started as a result of hiatus in sediment accumulation during marine flooding events (relative sea-level rise). Cement precipitation in these horizons continued through sediment burial as a result of organic-matter oxidation reactions in overlying organic-rich mudstones. The results of this study show a link between sedimentation (related to changes in relative sea level) and diagenesis, leading to the potential for the development of process-based, predictive models of early diagenesis in depositional successions.**

INTRODUCTION

Diagenesis exerts a major control on the physical and chemical properties of siliciclastic strata, and much attention has focused on developing models to understand and predict the occurrence and distribution of mineral cements (porosity reduction) and framework-grain dissolution (porosity increase). A predominant diagenetic feature in sandstones is carbonate cementation, taking the form of macroscopic, localized cement bodies having a variety of geometries, ranging from concretions to laterally persistent cemented zones (Bjørkum and Walderhaug 1990a, 1990b; Wilkinson 1991; McBride et al. 1995). In addition to forming prominent macroscopic features in sedimentary successions, carbonate cements also have a considerable economic impact on petroleum exploitation by significantly degrading reservoir quality and acting as barriers and baffles to fluid flow (Kantorowicz et al. 1987). In contrast to cementation, grain dissolution, depending on its occurrence and timing, may lead to enhancement of porosity and permeability within the strata and also may provide sources for mineral cements elsewhere in the succession. Given the prominent nature of these diagenetic features, and their economic impacts, the ability to understand and predict their distribution, size, and geometry is a significant benefit to predicting reservoir continuity in discrete depositional units.

To date, many models have been advanced to explain the origin and distribution of carbonate cements in siliciclastic successions. These include the distribution of shell material (Bjørkum and Walderhaug 1990a, 1990b), the presence of permeability heterogeneity in sandstones leading to localized increased migration of carbonate-bearing fluids (Prosser et al. 1993), and the occurrence of breaks in sediment accumulation during the development of marine flooding surfaces (Taylor et al. 1995).

In parallel to these diagenetic studies, high-resolution sequence stratigraphy has proven effective in understanding the stratigraphic evolution of stratal successions and in predicting the geometry and continuity of sandstone deposits in subsurface reservoirs (Van Wagoner et al. 1990). Despite obvious links, however, few studies have attempted to integrate detailed, high-resolution sequence-stratigraphic and diagenetic studies in order to develop predictive models for diagenetic alteration. This paper presents field and geochemical data for diagenetic features (carbonate cementation, detrital-grain leaching) in the Upper Cretaceous strata exposed in the Book Cliffs of Utah and Colorado. We describe the petrography and geochemistry of these carbonate cements and associated features and outline their relationship to the stratigraphic framework. On the basis of this study we propose mechanisms by which these diagenetic features formed. Moreover, direct integration of diagenetic analysis into large-scale stratigraphic studies appears to provide the best mechanism for the construction of process-based models of early diagenesis in siliciclastic successions.

GEOLOGICAL AND STRATIGRAPHIC SETTING

The Cretaceous Western Interior Seaway of North America stretched from the present Gulf of Mexico to the Arctic Ocean (Fig. 1). This foreland basin formed by crustal loading and flexural subsidence during thrusting and folding in the Cordilleran Orogen (Burchfiel et al. 1992). The Upper Cretaceous Blackhawk Formation and Castlegate Sandstone, which are described in this paper (Fig. 1), were deposited along the western margin of the Interior Seaway as a wedge of eastward-prograding siliciclastic strata (Hale and Van De Graaff 1964; Van De Graaff 1969, 1972), shed from the Sevier fold-and-thrust belt located to the west. Excellent exposure of the Book Cliffs provides an outstanding area to study large-scale geometry and stratigraphic architecture of stratal units, and hence, has resulted in numerous stratigraphic and sedimentological studies throughout this region (e.g., Fouch et al. 1983; Van Wagoner 1991, 1995; O'Byrne and Flint 1995; Taylor et al. 1995). The study presented here was carried out on the Grassy, Desert, and Castlegate strata in the Book Cliffs (Fig. 2). Marine shoreface sandstones and mudstones of the Grassy and Desert highstand systems tracts interfinger eastward and southward into the mudstone-dominated Mancos Shale. Each is overlain unconformably by the Desert and Castlegate lowstand systems tracts, respectively, truncating the highstand systems tracts toward the west (Fig. 2; Van Wagoner 1995). In addition to sequence boundaries, both marine flooding surfaces (parasequence boundaries) and transgressive surfaces (overlying lowstand systems tracts) can be traced for tens of kilometers in the outcrop.

* Present Address: Department of Environmental and Geographical Sciences, Manchester Metropolitan University, Chester Street, Manchester M1 5GD, U.K. E-mail: K.G.Taylor@mmu.ac.uk

JOURNAL OF SEDIMENTARY RESEARCH, VOL. 70, NO. 2, MARCH, 2000, P. 360–372
 1073-130X/00/070-360/$03.00

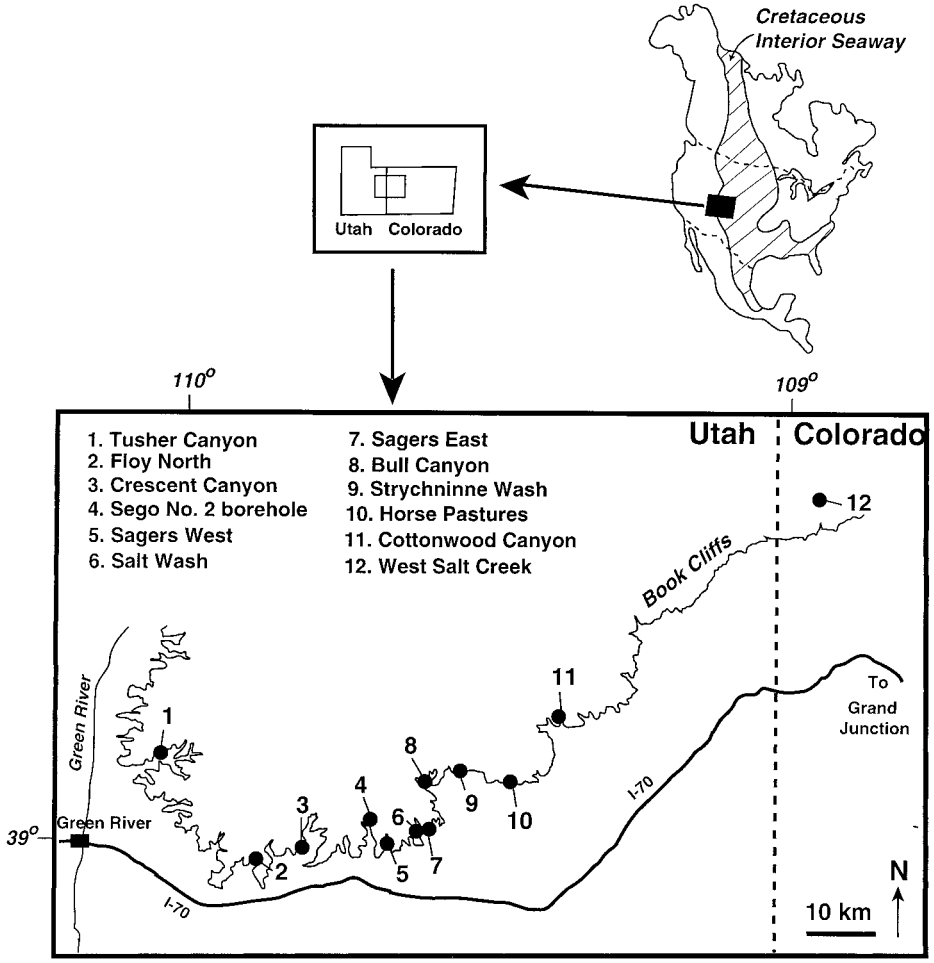

FIG. 1.—Location map showing the location of the outcrop exposures of the Upper Cretaceous strata in the Book Cliffs, Utah and Colorado. Locations mentioned in the text or used in Figure 2 are shown.

METHODS

Fresh, unweathered samples of cemented and uncemented sandstones were collected by hand from numerous outcrop localities along the Book Cliffs. Of these localities, twelve were the major focus of the analytical work (Fig. 2). In addition, material was sampled from two subsurface cores taken by the Exxon Production Research Company, each of which were located 0.5 km north of the natural outcrop. Polished thin sections of over 200 samples were prepared. After initial optical petrographic work in transmitted light the sections were coated with carbon and analyzed both petrographically and chemically in a Jeol 6400 Scanning Electron Microscope (SEM) equipped with a backscattered electron (BSE) detector. A fully quantitative Link eXL energy dispersive (ED) X-ray microanalysis system was used to determine major-element composition (Ca, Mg, Fe) of carbonate grains and cements within the samples. Trace-element contents (Sr, Mn) of carbonate minerals were determined on thin sections using wavelength-dispersive X-ray analysis on a Cameca electron microprobe. Detection limits for both of these elements was approximately 300 ppm.

Stable-isotope analyses were carried out at the Liverpool University Stable Isotope Laboratory. Powdered samples were heated in a low-temperature, oxygen-plasma oven for four hours to remove any organic matter. CO_2 gases were obtained by reacting approximately 3 mg of powdered sample with approximately 1 ml of anhydrous 100% orthophosphoric acid heated to 50°C. An acid fractionation factor of 1.01011 for dolomite and 1.00928 for calcite was used (values from those given by Friedman and O'Neil 1977, to account for 50°C reaction temperatures). Results were corrected by standard methods (Craig 1957) and calibrated using standard materials against the international standard NBS-19. They are expressed as per mil (‰) deviation from the V-PDB international standard (Coplen 1994, 1995). Sample reproducibilities in the laboratory are better than 0.1‰ for both carbon and oxygen values.

In almost all cases it was impossible to separate detrital dolomite from authigenic dolomite. Whenever possible, however, care was taken to analyze samples that contained only one phase of carbonate cement. Consequently, a value for detrital dolomite was obtained from those samples which contained no authigenic carbonate. In mixed detrital and authigenic samples the percentage by volume of detrital dolomite versus authigenic dolomite was determined through a combination of point counting on a petrographic microscope and element mapping on an SEM (which was possible because of the compositional difference between the detrital and authigenic dolomite). From these estimates, the value for the authigenic dolomite was calculated.

$^{87}Sr/^{86}Sr$ ratios for carbonate cements were measured at the University of Texas. Samples were crushed by hand in an agate mortar, with minimal grinding of detrital grains to limit the release of silicate Sr. Adsorbed surface Sr was removed with 1N ammonium-acetate exchange (an initial 8–10 hr followed by a second 1-hr exchange). Carbonate samples were reacted for 6–7 hr in 8% purified acetic acid, at room temperature (30 minutes for calcite samples). Dissolved material was separated from solids by centrifugation, concentrated by evaporation, and turned into nitrate salt with nitric acid. Raw data were corrected to give $^{87}Sr/^{86}Sr$ values for authigenic dolomite and detrital dolomite in the same way as for C and O isotope data described above.

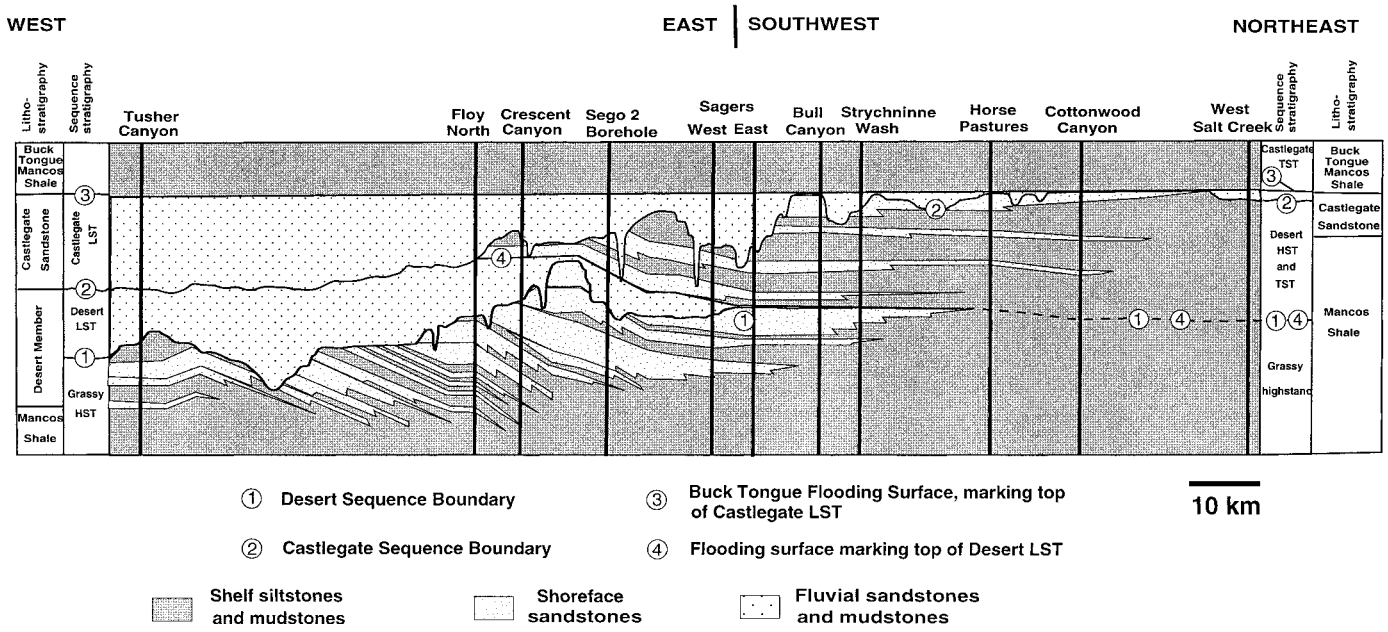

FIG. 2.—West-to-east cross section showing the lithostratigraphy and sequence-stratigraphic interpretation of the Grassy, Desert, and Castlegate depositional sequences in the Book Cliffs (after Van Wagoner 1995).

RESULTS

Outcrop-Scale Diagenetic Features

Both leached zones and carbonate-cemented bodies are present extensively within the Grassy, Desert, and Castlegate depositional sequences. These macroscopic diagenetic features are readily apparent in outcrop exposures, which have enabled detailed analysis of their form and geometry, and of their sedimentological and stratigraphic distribution. Three categories of outcrop-scale diagenetic features were recognized: (1) leached zones; (2) large isolated concretionary carbonate-cemented bodies; and (3) thin, laterally extensive carbonate-cemented zones. A summary of their outcrop-scale features is given here. A detailed account of their form, geometry, and stratigraphic distribution will be presented in a forthcoming paper.

''Whitecaps''.—Laterally extensive leached horizons, evident in the field as whitened, bleached zones (''whitecaps''), are present in proximal parts of the sequences, associated with coastal-plain and fluvial deposits. Individual ''whitecaps'' are generally present beneath coal beds, and in the cases where no coal is observed, the ''whitecap'' zones are overlain by an erosion surface, which has removed part of the original overlying deposits. The leached zones have vertical thicknesses of 5–10 m, and have lateral extents of up to 5 km. The ''whitecaps'' are more commonly observed in the highstand and lowstand systems tracts, particularly in the coastal-plain sediments deposited in the Grassy and Desert highstands systems tracts, and the fluvial sediments of the Desert and Castlegate lowstand systems tracts. At the bases of some ''whitecaps'', a thin horizon containing discrete, reddish brown siderite concretions is present. These concretions are generally 20 cm thick and up to 1 m long and are spaced up to 5 m apart. ''Whitecap'' horizons are also present in the subsurface cores (e.g., Sego No. 2 core; Van Wagoner et al., 1990), but can be detected only through petrographic analysis, because these horizons do not appear white in core.

Large, Isolated, Concretionary Carbonate-Cemented Bodies.—A prominent feature throughout the three sequences are large concretionary carbonate bodies. These concretions weather to a dark red-brown color and therefore can be mapped to delineate their form and distribution. The concretions range from 1 m to 8 m in vertical thickness, and are roughly spherical to horizontally elongate in form. They have a maximum long-axis diameter of 200 m, but more commonly extend up to 20 m. Although these concretions are prominent, they are not present throughout all the sandstones. They are exceedingly rare in proximal deposits (e.g., thick, amalgamated fluvial sandstones or thick, amalgamated upper-shoreface and foreshore strata). They are most predominant in highstand amalgamated shoreface sandstones (Figs. 3A, 4A), thin lowstand fluvial sandstones, or composite deposits of highstand shoreface and lowstand fluvial deposits (Figs. 3B, 4B). In such deposits their form and geometry appear to be strongly controlled by lithological heterogeneity in the sandstones. They are restricted to the coarser-grained parts of the sandstones and commonly follow major grain-size changes in the sandstones. For example, in thin, coarse-grained, fluvial channels that incised into distal lower-shoreface, interbedded fine-grained sandstones and siltstones, the concretions are bounded at their lower edges by the basal surface of the channel (e.g., the Desert Lowstand at Sagers Canyon West). However, in those thin fluvial channels that incised into amalgamated, lower-shoreface medium-grained sandstones (e.g., the Desert Lowstand at Salt Wash; Fig. 4B), the concretion bodies crosscut the sequence boundary. In the Grassy highstand, a number of high-frequency sequence boundaries have been recognized by Van Wagoner (1995). Carbonate concretions are present in shoreface sandstones immediately overlain by, and downdip from, these exposure surfaces (Fig. 3B). Concretions are generally absent from shoreface sandstones that are not associated with these high-frequency sequence boundaries (Fig. 3B). In many cases, compaction of sandstones around carbonate concretions can be observed.

Thin, Laterally Extensive, Carbonate-Cemented Zones.—These cemented bodies, although not as volumetrically significant as the large concretionary carbonate bodies, are equally prominent because of their distinctive form, geometry, and stratigraphic location. They have a maximum thickness of 3 m and have lateral extents of up to tens of kilometers. They are present exclusively beneath marine flooding surfaces, and are best developed beneath major transgressive surfaces (especially beneath the Buck Tongue flooding surface, which bounds the top of the Castlegate lowstand systems tract; Figs. 2, 4C, D). Although these cemented bodies are observed to be laterally continuous for hundreds of meters, more commonly they

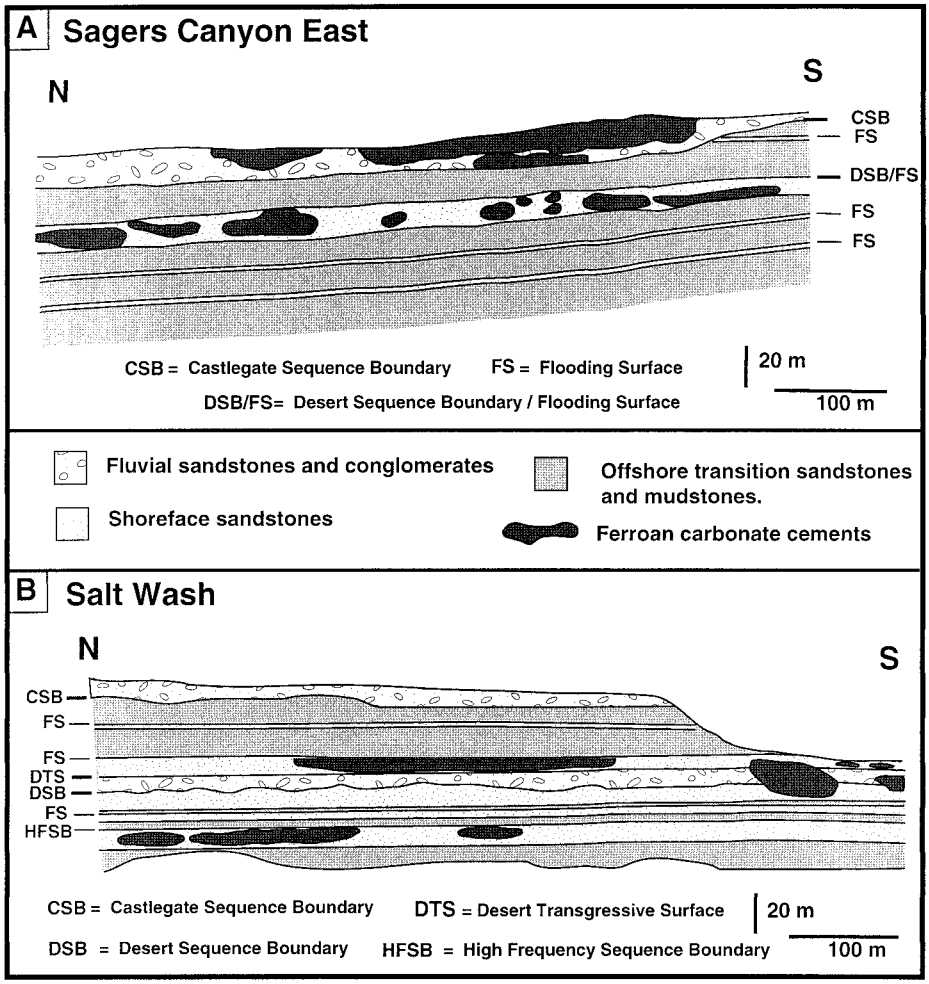

FIG. 3.—Diagrammatic sketches of outcrop exposures in the Grassy, Desert, and Castlegate depositional sequences, illustrating the occurrence and distribution of concretionary carbonate cemented bodies. **A)** Sagers Canyon East (east side of canyon). Note the presence of large, isolated concretionary carbonates in the amalgamated shoreface sandstones in the Grassy highstand (beneath the Desert Sequence Boundary/Flooding Surface; DSB/FS), and the presence of large, dolomite-cemented bodies in the fluvial sediments of the Castlegate lowstand (above the Castlegate Sequence Boundary (CSB). **B)** Salt Wash (east side of canyon). Note the presence of concretionary carbonate bodies in shoreface sandstones beneath a high-frequency sequence boundary (HFSB) in the Grassy highstand, and in the combined shoreface and fluvial sandstones of the Grassy highstand and Desert lowstand. Note also the absence of concretions in shoreface sandstones above the HFSB in the Grassy highstand.

take the form of individual roughly spherical, elongate cemented bodies separated by noncemented or poorly cemented sandstones. In the case of the best developed and most areally extensive example (beneath the Buck Tongue Flooding Surface), details of the cement geometry have been removed by modern-day surficial erosion. Hence, because of irregular topography, it is uncertain if the cemented zone is continuous or composed of separated cemented bodies. However, a clear lateral persistence can be observed in the distribution of the cemented bodies at this horizon. In many cases, the upper surfaces of these cemented horizons contain an intensely bioturbated interval that contains unlined vertical burrows (a *Glossifungites* ichnofacies containing *Skolithos* burrows; Fig. 4D) suggesting that a firm substrate may have developed shortly after deposition.

Petrography and Geochemistry of Diagenetic Features

Background Petrography and Diagenesis.—Monocrystalline quartz is the predominant framework grain throughout the Book Cliffs sandstones. Lithic grains of chert, volcanic, and metamorphic rocks are also common. A significant component of all the sandstones are detrital dolomite grains, which are rounded to subangular and have a grain size similar to the associated detrital quartz grains (Fig. 5A). From point-count data, the percentage of detrital dolomite grains averages 10 volume percent of the sandstones (equating to up to 15% of framework grains). Similar proportions of detrital dolomite have been recognized from other Upper Cretaceous Western Interior Seaway strata in Alberta (McKay et al. 1995). All detrital dolomite is nonferroan, stoichiometric dolomite with Sr concentrations of less than 300 ppm. It has an average $\delta^{13}C$ of +0.3‰ VPDB, an average $\delta^{18}O$ of −4.6‰ VPDB, and an average $^{87}Sr/^{86}Sr$ value of 0.7092 (Table 1; Figs. 6, 7). It also has a chemical and isotopic signature that is different than any of the dolomite cements in the sequences (Table 1). In sandstones lacking cement, the predominant authigenic minerals are quartz overgrowths, kaolinite, and late-stage calcite (Fig. 5B, C). Also, partial dissolution of lithic fragments and feldspar grains is common in uncemented sandstones, a phenomenon rarely observed in carbonate-cemented sandstones.

''Whitecaps''.—Petrographically and mineralogically, sandstones constituting the ''whitecap'' horizons are devoid of detrital dolomite (and other carbonate) grains, which is an abundant component of the sandstones throughout other parts of the Book Cliffs succession. ''Whitecap'' thicknesses, and associated zones of dissolution of detrital dolomite, range from 5 to 10 m (Fig. 8). Detrital feldspar contents are also lower in sandstones within ''whitecaps'' than away from them, with detrital feldspar absent for a distance of up to 5 m below coal beds.

At the bases of some of the ''whitecap'' horizons are reddish-weathering siderite concretions, forming discrete concretions along individual zones. This siderite cement is a minor component of the sandstone, and occurs as small (5 μm) rhombs rimming detrital grains (Fig. 5D). This siderite cement is enveloped by quartz overgrowths and therefore predated quartz cement in the sandstones.

Large, Isolated Concretionary Carbonate-Cemented Bodies.—Ferroan dolomite is the predominant mineral cement in these cemented bodies.

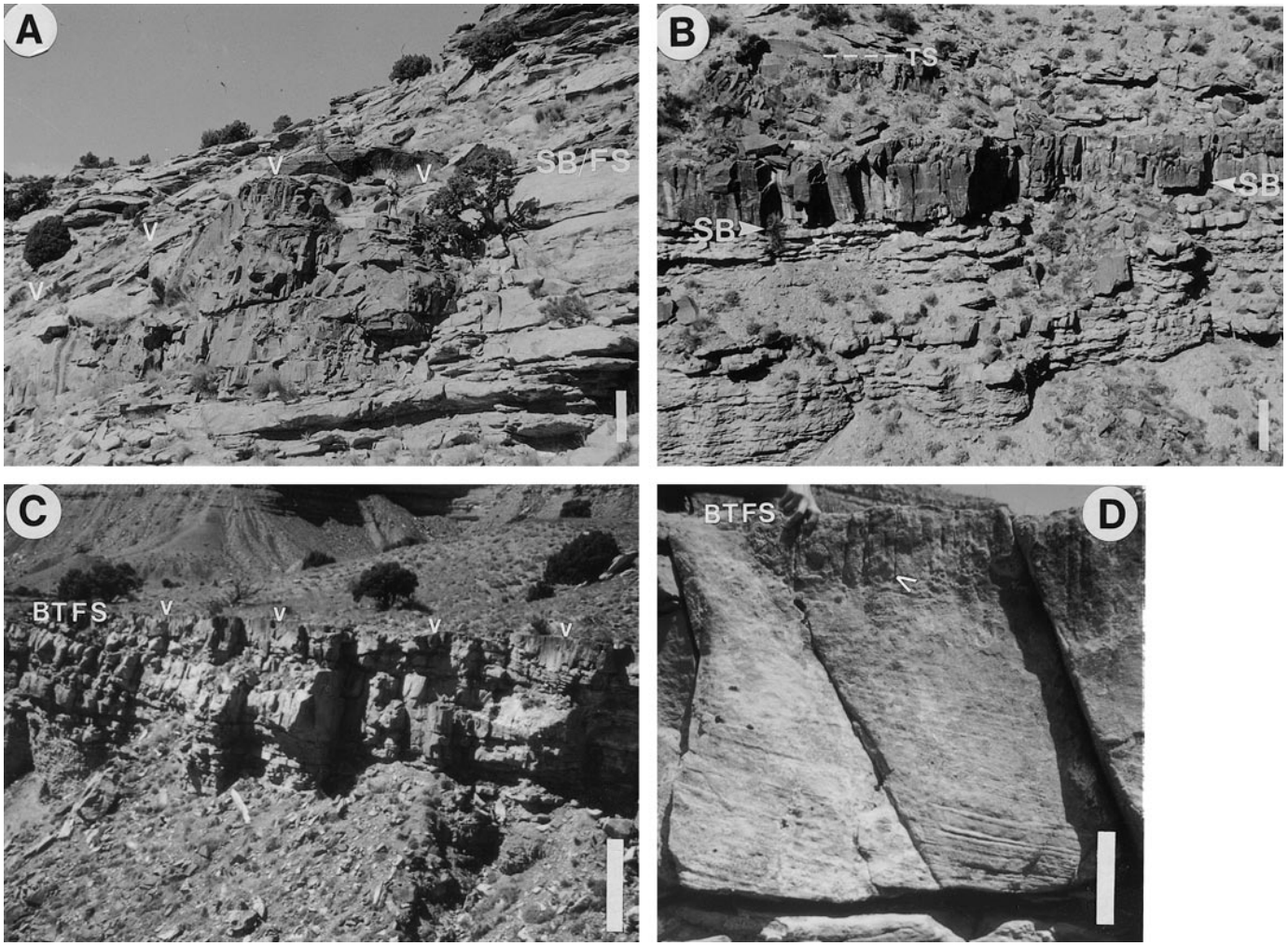

FIG. 4.—Outcrop photographs of carbonate-cemented bodies in the Book Cliffs succession. **A)** Large carbonate concretion in amalgamated lower-shoreface sandstones in the Grassy highstand at Sagers Canyon East. SB/FS = Desert sequence boundary/flooding surface (outcrop extent arrowed). Scale bar = 2 m. **B)** Large, concretionary carbonate-cemented body in the thin, fluvial Desert lowstand at Sagers Canyon West. SB = Desert sequence boundary; TS = Desert transgressive surface. Note the absence of carbonate cement in the thin, lower-shoreface sandstones of the Grassy highstand below. The lower boundary of the carbonate cement body at this location correlates to the increase in grain size above the Desert sequence boundary. Scale bar = 2 m. **C)** Thin, laterally extensive cement zone (arrowed) beneath the Buck Tongue flooding surface (BTFS; upper boundary of the Castlegate lowstand) at Horse Pastures. Scale bar = 5 m. **D)** Unlined, vertical borrows of a *Glossifungites* ichnofacies in trough cross-bedded fluvial sandstones of the Castlegate lowstand, directly beneath the Buck Tongue flooding surface (BTFS). One burrow is arrowed. Scale bar = 0.5 m.

The style of cementation varies within individual cemented bodies. Throughout the concretions, ferroan dolomite cement totally occludes porosity, constituting approximately 40% intergranular volume (Figs. 5E, 9). There is little evidence of grain replacement or corrosion by cements, and therefore these dolomite-cemented sandstones are inferred to have the approximate intergranular porosity at the time of deposition. In addition to this high intergranular volume, detrital grain contacts are predominantly point–point in nature, and there is a general absence of long face contacts (Fig. 5E). Quartz, kaolinite, and late calcite cements, which are abundant in sandstones away from cemented zones (Fig. 5B, C), are absent from these cemented bodies. Although most of the cemented bodies are characterized by high intergranular volumes of porosity-occluding cements, at the edges of cemented bodies thin zones are present where ferroan dolomite does not totally occlude porosity, and quartz cement and primary porosity

→

FIG. 5.—**A)** Thin-section photomicrograph showing detrital, monocrystalline, nonferroan dolomite (d) in uncemented sandstone. This detrital, inclusion-rich dolomite grain has an inclusion-free, authigenic dolomite overgrowth (arrowed). Field of view = 250 μm. **B)** Late calcite cement (c) in sandstone away from dolomite cement zone. Note that the calcite cement postdates quartz overgrowth formation (q). Field of view = 300 μm. **C)** Authigenic kaolinite (k) in an uncemented sandstone. Field of view = 130 μm. **D)** Early siderite rhombs (s), predating quartz overgrowth cement, in sandstone at base of leached zone that underlies a coal bed. Field of view = 150 μm. **E)** Thin-section photomicrograph of early, ferroan-dolomite cement (fd) in the central part of a large, isolated dolomite-cemented body. Note the high cement volume, the point–point contacts of detrital quartz grains (q), and the early diagenetic pyrite (p). Field of view = 500 μm. **F)** Later, ferroan dolomite cement (fd2) from outer part of large isolated concretion, precipitated on a less ferroan dolomite cement (fd1). Note presence of preserved primary porosity (p). Field of view = 400 μm. **G, H)** Zoned carbonate cement in laterally extensive cement zone beneath the Buck Tongue flooding surface. Note the detrital nonferroan dolomite core (d), surrounded by a thin zone of ferroan dolomite, calcite with pyrite (c), and further ferroan dolomite (fd). Field of view = 300 μm.

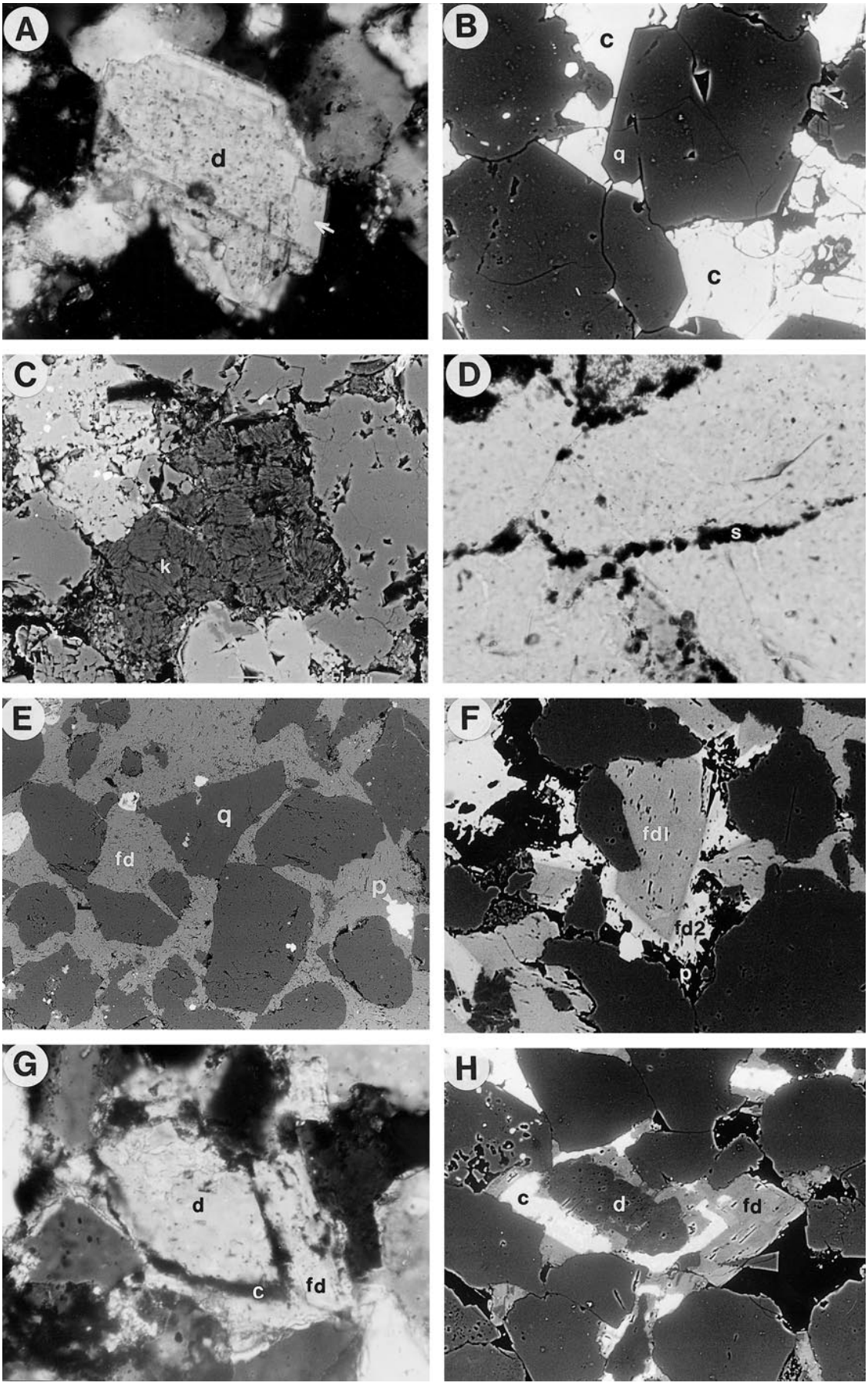
A
d
B
c
q
c
C
k
D
s
E
q
fd
p
F
fd1
fd2
p
G
d
c
fd
H
c
d
fd

TABLE 1.—*$\delta^{13}C$, $\delta^{18}O$, and $^{87/86}Sr$ data for carbonate cement components and detrital dolomite grains within selected samples from Book Cliffs.*

	Sample	$\delta^{13}C$ ‰ VPDB	$\delta^{18}O$ ‰ VPDB	$^{87/86}Sr$	Corrected $\delta^{13}C$ ‰ VPDB	Corrected $\delta^{18}O$ ‰ VPDB	Corrected $^{87/86}Sr$
Concretionary carbonates—early dolomite cement	SEG-13	2.55	−6.96	0.707938	3.3	−7.8	0.707806
	SEG-13a	1.07	−8.88	0.707998	1.3	−10.3	0.707872
	SEG-14	0.24	−10.09	0.708043	0.2	−12.0	0.707933
	SEG-15a	2.15	−7.21	0.708109	2.8	−8.1	0.707918
	SA2-9	−1.77	−9.08	0.708149	−2.5	−10.6	0.708057
	SCW-8	2.01	−8.04	0.707909	2.6	−9.2	0.707805
	SEG-14a	−0.25	−9.50	n.d.	−0.4	−11.2	n.d.
	SEG-15	0.03	−9.00	n.d.	−0.1	−10.5	n.d.
	SCW-6	0.96	−8.59	n.d.	1.2	−10.0	n.d.
	SCW-7	2.63	−7.50	n.d.	3.4	−8.5	n.d.
	SA3-8a	−0.55	−8.53	n.d.	−0.8	−9.9	n.d.
	SA3-8b	−0.49	−8.05	n.d.	−0.8	−9.2	n.d.
Concretionary carbonates—later dolomite cement	SEG-11a	−2.90	−10.30	0.709266	−4.5	−13.3	0.709268
	SEG-11b	−3.52	−11.52	0.709294	−5.5	−15.1	0.709302
	SEG-12	−3.65	−10.80	0.709161	−5.7	−14.0	0.709140
	SA2-10	−2.26	−10.51	0.708867	−3.1	−12.5	0.708818
	SCW-15	−2.85	−10.50	n.d.	−3.9	−12.5	n.d.
	SA2-8	−3.33	−10.12	n.d.	−4.5	−12.0	n.d.
Laterally extensive cement bodies—dolomite cement	CC52	−2.15	−9.19	0.709291	−3.8	−12.3	0.709313
	TCA-29	−3.92	−11.36	0.710685	−6.7	−15.9	0.711637
	ETW-1a	−3.93	−10.61	0.710348	−6.8	−14.7	0.711075
	STUB-1	−2.96	−9.54	0.710272	−5.1	−12.9	0.710948
	CQW-12	−3.18	−10.17	0.709062	−5.5	−14.0	0.709006
Detrital dolomite	FN-3	0.30	−4.44	0.709374	0.3	−4.4	0.709374
	FN-5	0.31	−4.77	0.709343	0.3	−4.8	0.709343
	SEG-24	n.d.	n.d.	0.709055	n.d.	n.d.	0.709055
Late calcite cement	SEG-29	−7.14	−16.02	0.711072	−7.1	−16.0	0.711072

The raw isotope data represent whole-sample analyses (a mixture of cement and detrital carbonate), and the "corrected" data for carbonate cements represent the calculated value for the cement component alone, following correction for the presence of detrital dolomite.

are also present (Fig. 5F). In these outer zones porosity, which ranges from 5 to 10 volume percent, is preserved and dolomite cement forms approximately 10–25 volume % of the sandstone (Fig. 9).

In addition to the petrographic textures, there are clear contrasts in composition between the porosity-occluding dolomite cements forming the bulk of the concretions and the dolomite cements at the concretion edges. The concretion cores have low Fe contents (2–5 mol %; Figs. 9, 10), whereas cements on the outer edge are more Fe-rich (8–14 mol %; Figs. 9, 10). Mn contents mirror the changes in Fe contents, such that cements in concretion centers have Mn contents in the range 0 to 400 ppm, and the outer cements contain 300 to 1500 ppm Mn. Sr contents of dolomite cements are high, up to 1000 ppm, in the central parts of cement zones, falling to 300 ppm or less in the outer parts of concretions. Some concretions exhibit asymmetrical changes in cement volume and cement composition (e.g., Fig. 9).

$\delta^{13}C$ and $\delta^{18}O$ values for dolomite cement also exhibit systematic changes. $\delta^{13}C$ values for dolomite cements in the concretion cores are centered around 0‰ (-2.5 to +3.4‰ VPDB; Table 1; Figs. 6, 7). $\delta^{18}O$ values for the same cements are negative (-7.8 to −12.0‰ VPDB; Table 1; Figs. 6, 7). These contrast with values for dolomite cements in the outer parts of concretions, for which both $\delta^{13}C$ and $\delta^{18}O$ values are significantly lower ($\delta^{13}C$ = −3.1 to −5.7‰ VPDB; $\delta^{18}O$ = −12.0 to −15.1‰ VPDB; Table 1; Figs. 6, 7). There is a strong positive correlation between $\delta^{13}C$ and $\delta^{18}O$ (Fig. 6). $^{87}Sr/^{86}Sr$ data for the cements show an increase from 0.7078 in the central parts to 0.7093 in outer parts (Table 1; Fig. 7). $^{87}Sr/$

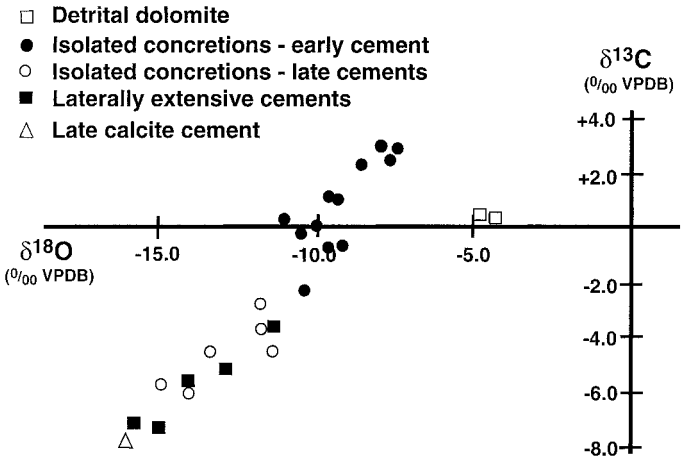

FIG. 6.—Plot of $\delta^{13}C$ vs. $\delta^{18}O$ for large isolated concretion cement, laterally extensive cements, detrital dolomite, and late calcite.

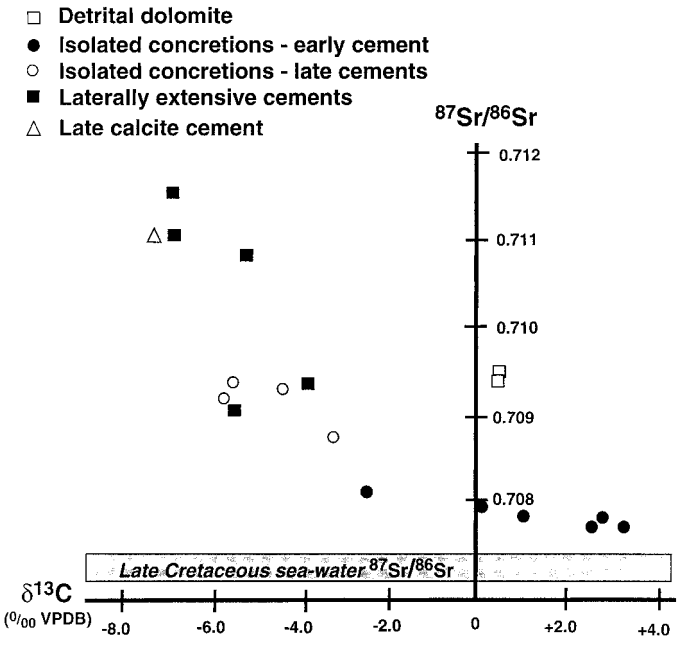

FIG. 7.—Plot of $\delta^{13}C$ vs. $^{87}Sr/^{86}Sr$ for large isolated concretion cement, laterally extensive cements, detrital dolomite, and late calcite. Late Cretaceous seawater $^{87}Sr/^{86}Sr$ is indicated by a shaded bar (from Burke et al. 1982).

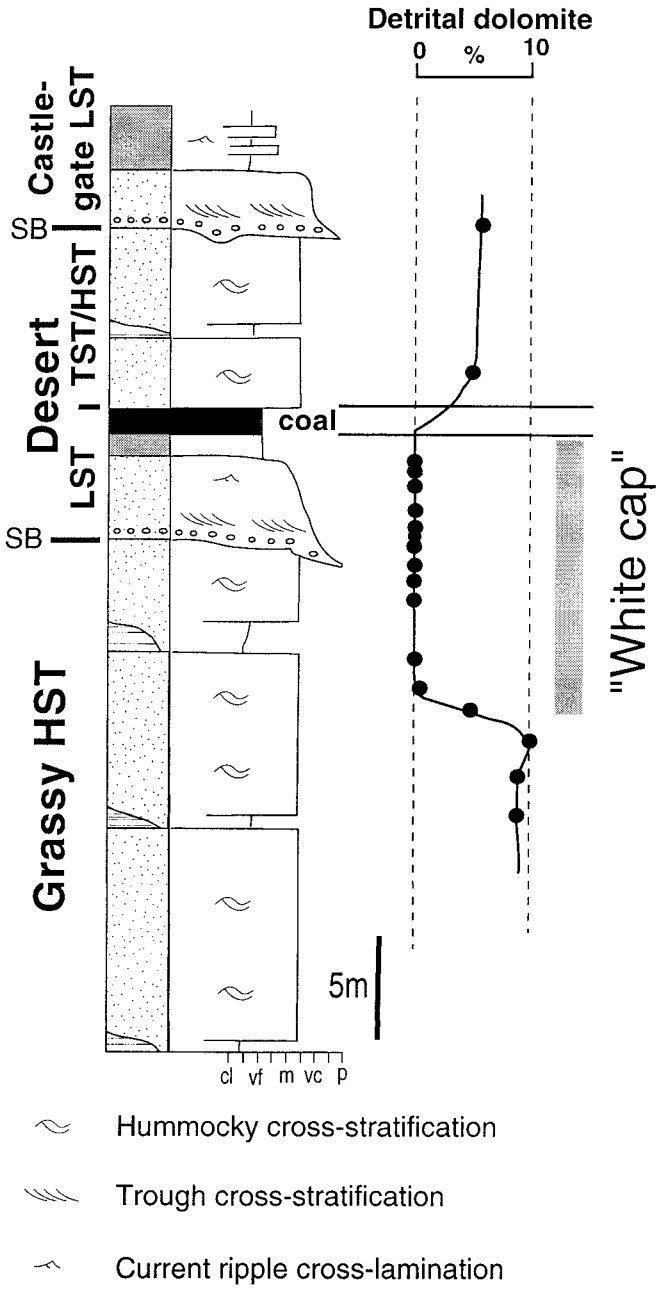

FIG. 8.—Detrital carbonate contents in sandstones associated with a coal horizon, Grassy HST and Desert LST, Sego No. 2 core (see Van Wagoner et al. 1990). Note the absence of detrital dolomite in sandstones up to 10 meters beneath the coal horizon.

^{86}Sr values are inversely correlated with $\delta^{13}C$ values for the cements as a whole (Fig. 7).

Thin, Laterally Extensive Carbonate-Cemented Zones.—Laterally extensive carbonate cements are petrographically distinct. They are predominantly ferroan dolomite but, unlike in the large isolated concretions, the cements do not totally occlude porosity. Ferroan dolomite has overgrown detrital, nonferroan dolomite grains in optical continuity (Fig. 5G, H). In some cases these cements are zoned, with initially ferroan dolomite, then calcite and pyrite, and finally ferroan dolomite (Fig. 5G, H). In pores away from carbonate cement overgrowths, quartz cement is common, along with preserved primary porosity.

Dolomite cements in these laterally extensive cement bodies have Fe contents of 3–6 mol % and Sr contents of approximately 300 ppm or less. $\delta^{13}C$ values of the cements range from −3.8 to −6.8‰ VPDB, whereas the $\delta^{18}O$ values range from −12.3 to −15.9‰ VPDB (Table 1; Fig. 6). $^{87}Sr/^{86}Sr$ ratios for the cements range from 0.7093 to 0.7116 (Table 1; Fig. 7).

DISCUSSION

''Whitecaps'' (Leached Zones)

In the light of the abundance of detrital dolomite in strata throughout the Book Cliffs succession, it can be assumed that detrital carbonate was also originally present in the deposits that now form the ''whitecaps'' and was subsequently removed some time after deposition. Petrographic analysis of these sandstones reveals the absence of oversized pores, which may indicate that dissolution of detrital dolomite was an early diagenetic process that took place prior to sediment compaction.

Such early dissolution of detrital dolomite (and other detrital carbonates) was probably associated with release of acidic fluids from the overlying coal-bearing intervals following deposition and during early sediment burial and compaction. Organic-acid generation from coals during burial and mineral leaching in underlying sediments has been well documented (e.g., Percival 1983; Van Keer et al. 1998). Organic acids have also been generated as a result of organic-matter oxidation reactions in landfill sites shortly after deposition (Manning 1997; Manning and Bewsher 1997). Such early postdepositional organic-acid generation is also likely within coals. Of the detrital framework grains in the Book Cliffs strata, detrital dolomite would be most affected by these organic-rich acid solutions, resulting in leaching of the grains from sandstones immediately beneath the coals. Detrital feldspar grains have also been leached from these horizons, but only to depths of approximately 5 m beneath coal beds. The role of organic acids in the dissolution of feldspar has been proposed and documented experimentally (Surdam et al. 1989; Manning et al. 1992, 1994). Variations in vertical extent of dissolution of detrital feldspar and detrital dolomite most likely reflects the relative resistance of feldspars to organic-acid dissolution compared to dolomite. Dolomite leaching is not observed beneath sequence boundaries, indicating that meteoric fluids alone were not responsible for dissolution of detrital dolomite.

Large, Isolated Concretionary Carbonate-Cemented Bodies

Cement Timing and Composition.—Preservation of intergranular space (up to 40%) in the concretions, the general absence of detrital grain replacement textures, and the absence of later cements that are typical in sandstones away from cemented zones indicate that the dolomite cement formed during early burial of the sandstones, prior to significant compaction. By comparison with published compaction curves for sandstones (e.g., Baldwin and Butler 1985), cement precipitation within the first 200 m of burial is inferred. However, the presence of dolomite cements alongside quartz cement in outer zones of concretions and the preservation of porosity suggest that cementation continued through later burial. We therefore propose that the dolomite cements in the margins of the concretions formed during later burial.

The Fe content of the dolomite cement in the concretions increases from 2–5 mol % for early cements to 8–14 mol % for later cements. An explanation for this trend is that Fe contents in porewaters increased during sandstone burial, as a result of increased supply of Fe(II) to pore waters through the reduction of Fe(III) residing in iron oxides and iron silicates. Previous studies have documented that Fe(III) reduction proceeds throughout diagenesis as a result of Fe(III)-containing minerals having differing reactivities (Canfield et al. 1992; Postma 1993). Increasing Mn contents in the dolomite cements can also be explained by this mechanism.

The marked change in Sr content of cements during burial can be ex-

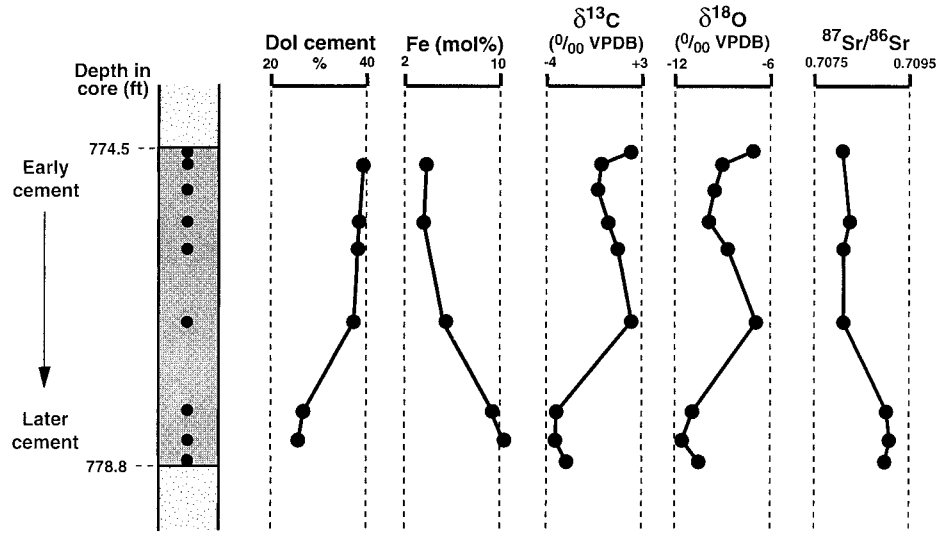

FIG. 9.—Traverse across a large isolated cement concretion in the Grassy highstand systems tract in Sego No 2 core. Note that the concretion is not symmetrical and that the earlier parts, represented by the higher dolomite cement volumes, dominate the upper parts of the cement body. Note the increase in Fe and $^{87}Sr/^{86}Sr$, and the decrease in $\delta^{13}C$ and $\delta^{18}O$ in later cements (i.e., from the upper parts to the lower parts of the concretion).

plained by a different mechanism. Unlike Fe and Mn, Sr contents are high in early cements (up to 1000 ppm), with later cements falling to 300 ppm or less. However, only the earliest parts of concretions contain high Sr contents, indicating that Sr concentrations in pore fluids decreased relatively quickly during sandstone burial. High Sr contents can be supplied to porewaters by early diagenetic dissolution of aragonitic shell material (Tucker and Wright 1990). We propose a similar mechanism for the Cretaceous strata of the Book Cliffs, with early dissolution of aragonitic shell material leading to high Sr contents in porewaters. After complete dissolution of aragonitic shell material, porewater Sr concentrations decreased and dolomite cement with low Sr content was precipitated.

C and O Stable Isotopes: Constraints on Cement Source and Porewater Composition.—Early dolomite cements are isotopically distinct from later dolomite cement (Table 1; Fig. 6). $\delta^{13}C$ values for early cements of −2.5 to +3.4‰ VPDB suggest a carbon source dominated by marine carbonate. $\delta^{18}O$ values (-7.8 to −12‰) are more equivocal. Given that petrographic evidence indicates early dolomite precipitation with no evidence for recrystallization of the cements, we reject the possibility of burial recrystallization of cement to account for these light $\delta^{18}O$ values. Furthermore, there is no direct evidence for an ^{18}O-depleted Western Interior Seaway in the Utah–Colorado area at this time. Isotopic analysis of early diagenetic dolomite cements from the Mancos Shale in Colorado at a stratigraphic horizon similar to this study (Klein et al. 1999) shows $\delta^{18}O$ values from the earliest cements close to SMOW, suggesting that, at least locally, the Western Interior Seaway waters were not significantly lighter that mean ocean values. If dolomite precipitation from marine fluids is assumed (Late Cretaceous seawater = −1.2‰ SMOW; Shackleton and Kennett 1975), the $\delta^{18}O$ values for the cement would indicate precipitation at temperatures of 62–92°C (using the fractionation equation of Matthews and Katz 1977) (Fig. 11). Under normal burial-temperature gradients (30°C/km) and a bottom water temperature of 10°C, this would suggest precipitation at burial depths of approximately 2–3 km, which is not supported by the petrographic observations.

We propose that the cements precipitated from meteoric waters. Although there are no direct data for the meteoric-water composition in the study area, McKay et al. (1995) calculated a $\delta^{18}O$ value of −15‰ SMOW for the higher-latitude Cretaceous Western Interior Seaway strata in Canada. Similarly, Hendry et al. (1996) conclude that Cretaceous meteoric water in the North Sea (a mid-latitude setting) was at least as negative as −8‰ SMOW. On the basis of these data, we have assumed a $\delta^{18}O$ value of −10‰ SMOW to be reasonable for meteoric fluids in the Book Cliffs area during the Late Cretaceous. For a $\delta^{18}O$ water composition of −10‰ SMOW, precipitation temperatures for the early dolomite cements of 18–38°C are indicated (Fig. 11). These near-surface to shallow-burial temperatures are more consistent with the petrographic features present in the concretions.

Both $\delta^{13}C$ and $\delta^{18}O$ values for later dolomite cements in the isolated concretions are significantly lower than those for early cements ($\delta^{13}C$ =

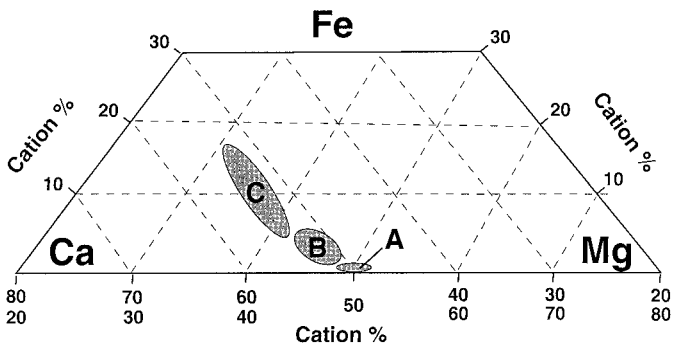

FIG. 10.—Chemical composition of detrital dolomite grains and dolomite cements in concretionary carbonate bodies (Ca, Mg, and Fe plotted as cation %). A = detrital dolomite grains; B = early dolomite cements; C = later dolomite cements.

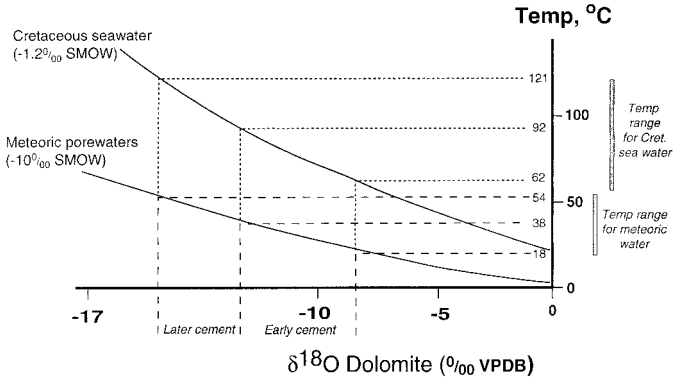

FIG. 11.—Plot of $\delta^{18}O$ vs. temperature for the early and later ferroan dolomite cements of large isolated cement bodies. Curves for both Cretaceous marine water and meteoric porewaters are shown (based on the fractionation equation of Matthews and Katz 1977).

−3.1 to −5.7‰ VPDB; $\delta^{18}O$ = −12.0 to −15.1‰ VPDB; Table 1). The lower $\delta^{13}C$ values for later cements are consistent with marine carbonate continuing to be a predominant cement source during burial diagenesis, but with a significant component of organic-matter-derived carbonate, possibly derived from decarboxylation reactions in the adjacent Mancos Shale. The low $\delta^{18}O$ values are also consistent with precipitation from evolved meteoric fluids at slightly elevated temperatures (38–54°C) associated with sediment burial (Fig. 11). Thus, both $\delta^{13}C$ and $\delta^{18}O$ variations within the concretionary cement bodies are consistent with continued precipitation during progressive burial.

$^{87}Sr/^{86}Sr$ Constraints.—$^{87}Sr/^{86}Sr$ values for early cements are slightly greater than Late Cretaceous seawater (0.70725–0.7075; Burke et al. 1982) (Fig. 7). The later cements in the concretions have yet greater values (Table 1, Fig. 7). Because fractionation of $^{87}Sr/^{86}Sr$ does not occur during mineral precipitation, the fluids from which the carbonate cements precipitated had a $^{87}Sr/^{86}Sr$ composition more elevated than Late Cretaceous seawater. The higher $^{87}Sr/^{86}Sr$ values for cements are best interpreted as resulting from precipitation from modified marine pore fluids. Breakdown of detrital feldspar and lithic fragments could increase ^{87}Sr in the pore waters. However, petrographic observations suggest that where such breakdown has occurred it is restricted to sandstones outside carbonate concretions. Within carbonate concretions dissolution is minimal. This indicates that dissolution of detrital grains occurred predominantly after early cement precipitation and, therefore, local grain dissolution could not be the source of ^{87}Sr for the early dolomite cements. In addition, feldspar contents within the sandstones are generally low (maximum of 3 percent). Another source for ^{87}Sr could be addition of a meteoric-water component to the pore waters, which is indicated from the $\delta^{18}O$ data (see above). Meteoric waters generally have a high $^{87}Sr/^{86}Sr$ because of input of ^{87}Sr from mineral dissolution (Faure et al. 1963). This is a plausible mechanism for elevation of the porewater $^{87}Sr/^{86}Sr$. A third source of ^{87}Sr might be dissolution of detrital dolomite grains, which have a high $^{87}Sr/^{86}Sr$ value (Table 1; Fig. 7). In addition, dissolution of shell material would have moderated the above mechanism inasmuch as it would be expected to have the same composition as Late Cretaceous seawater. The $^{87}Sr/^{86}Sr$ values for the earlier cements are between those of detrital dolomite and Late Cretaceous seawater (detrital shell material). Given that the earlier cements have elevated Sr concentrations (Fig. 9), it is therefore likely that $^{87}Sr/^{86}Sr$ values for early dolomite cements resulted from a combination of a meteoric component to the pore waters and dissolution of detrital dolomite and shell material, with possibly an input from detrital feldspar. The higher $^{87}Sr/^{86}Sr$ values for the later dolomite cements is consistent with precipitation from pore fluids that have undergone modification with respect to $^{87}Sr/^{86}Sr$ during later burial through burial dissolution of detrital feldspar and lithic grains.

Source of Carbonate for Cements.—$\delta^{13}C$ data indicate that marine carbonate was a major source for the carbonate cements in the sandstones. For the case of the early dolomite cements this source appears to be the only significant component, whereas later dolomite cements had a significant contribution from organic matter via decarboxylation reactions. Two potential reservoirs of ''marine'' carbonate in the Book Cliffs sequences are primary shell material and detrital dolomite, both of which have been observed in the succession. Shell material is rare at present, mainly restricted to fluvial/estuarine channel lags (see Van Wagoner 1995), and is generally replaced by dolomite. Relict dissolution voids are rare. It is hard to estimate depositional amounts of shell material. However, the size and abundance of large-scale dolomite-cemented bodies in the successions (which commonly occupy up to one-third by volume of 10-m-thick amalgamated shoreface sandstones) would seem to require significantly more carbonate than could be supplied by the inferred amounts of shell material. Furthermore, if primary shell material, either internally or externally derived, had been the source for dolomite cements, a source for the Mg in the dolomite would also need to be invoked. Potential Mg sources could be sea water or clay-mineral reactions. It is improbable, however, that these sources could have provided the large amounts of Mg required for the cements. Hence, shell material is inferred to have been a minor source for the dolomite-cemented bodies in the Book Cliffs succession.

A far more abundant source of carbonate in the succession is detrital dolomite grains. This detrital dolomite has $\delta^{13}C$ values consistent with a ''marine'' carbonate, and it would also have formed a source for the Mg in the dolomite cements. Petrographic data show that detrital dolomite grains have remained unaltered throughout most of the sandstones. As discussed previously, however, early diagenetic dissolution of detrital dolomite took place in ''whitecap'' horizons beneath coal beds (Fig. 8). We infer that this dissolution of detrital dolomite was a major source of carbonate for the dolomite-cemented bodies in the Book Cliffs strata.

Transport of Carbonate.—In the Book Cliffs sequences coal beds are present in highstand and lowstand strata deposited in coastal-plain environments during times of lowered relative sea level. During times of sea-level fall the freshwater hydraulic head may increase, potentially resulting in ingress of meteoric waters into more distal sediment packages (Machemer and Hutcheon 1988). In the case of the Book Cliffs succession these meteoric fluids would have contained carbonate derived from dissolution of detrital carbonate grains from beneath coal horizons. $\delta^{18}O$ data for carbonate cements strongly suggests that pore fluids at the time of precipitation had a meteoric water component. Field analysis shows that the large concretions occur in major sandstones and that their form is commonly controlled by lithofacies heterogeneity (e.g., cements are restricted to the basal parts of fluvial channels). Both of these observations suggest that large-scale fluid flow was an important process in the precipitation of these cements and support the hypothesis that carbonate was imported to the sites of precipitation by ingress of meteoric fluids. The presence of carbonate concretions in shoreface sandstones downdip from high-frequency sequence boundaries in the Grassy highstand (Fig. 3B), and the absence of concretions in other shoreface sandstones, further supports the interpretation that meteoric fluids transported carbonate into the sandstones during times of relative sea-level fall. The formation of carbonate-cemented bodies parallel to groundwater flow directions has been documented by both McBride et al. (1994) and Mozley and Davis (1996). Unfortunately, the nature of the exposure in the Book Cliffs (dominated by large cliffs) does not allow such detailed assessment of the three-dimensional geometry of individual cement bodies. The presence, in some cases, of asymmetrical concretion growth away from lithofacies boundaries (Fig. 9) also supports a large-scale fluid-flow component to solute transport.

Cement Precipitation Mechanisms.—A carbonate source and a transport mechanism has been identified above for the carbonate cements (Fig. 12A). As meteoric fluids containing dissolved carbonate (and Ca and Mg) ingressed into more distal parts of the succession, they became mixed with the existing marine pore waters. As a result, the fluids became supersaturated with respect to dolomite, and dolomite cement precipitation occurred, with nucleation taking place on detrital dolomite grains. In addition to Ca and Mg supplied by dissolution of detrital dolomite in up-dip locations, Fe present in dolomite cement must have been supplied by an additional source. Fe(II) is supplied to pore waters during early diagenesis by Fe(III) reduction. This reaction leads to an increase in pH (Coleman 1985) and can significantly decrease the solubility of carbonates in pore waters. Precipitation of dolomite cement, therefore, was probably a result of the combination of both meteoric fluid evolution through mixing with marine pore waters, and pH increase through Fe(III) reduction.

Laterally Extensive Cemented Zones

Timing.—Carbonate cements in the thin laterally extensive cemented zones do not fully occlude porosity, and therefore the timing of cementation is poorly constrained. In the cemented zones, ferroan dolomite and calcite overgrowths are present around detrital dolomite grains (Fig. 5G, H), whereas away from these grains, quartz cements are common along with

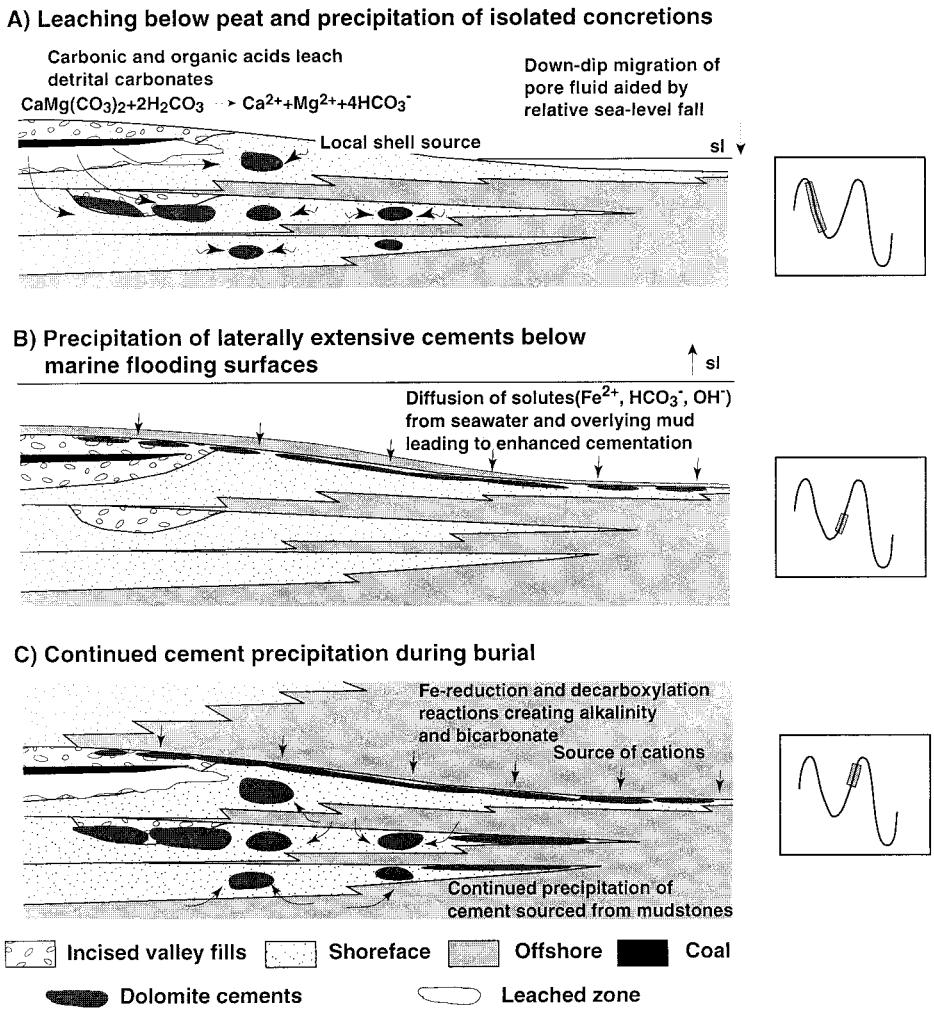

FIG. 12.—Summary diagram of the diagenetic mechanisms controlling the formation of carbonate cements in the Upper Cretaceous Book Cliffs strata. **A)** Downward-percolating groundwaters, enriched in organic acids, beneath coal horizons dissolve detrital dolomite in sediments. During times of lowered relative sea level these fluids migrated along high-permeability units (amalgamated shoreface sandstones, fluvial sandstones, and amalgamated shoreface/fluvial sandstones). As these fluids evolved by mixing with existing marine pore fluids, cement precipitation in the form of concretionary bodies resulted. In addition, unstable shell material underwent dissolution and provided a local source of carbonate in these sandstones. **B)** During times of sea-level rise (marine flooding events) a rapid increase in accommodation space led to a period of depositional hiatus. As a result sediment residence times in early diagenetic zones increased, leading to the initial precipitation of early carbonate cement. **C)** During subsequent burial of the sediments, organic-matter oxidation reactions (iron reduction, decarboxylation) in the organic-rich mudstones overlying the marine flooding surface led to the continued precipitation of carbonate cements in sandstones beneath the marine flooding surface. As a result of (B) and (C), laterally extensive carbonate cemented zones formed.

preserved primary porosity. In contrast to the concretionary cement bodies, the presence of overgrowths of zoned ferroan dolomite and calcite cement on detrital nonferroan dolomite grains suggests relatively slow cement precipitation. This is supported by the nature of discrete zones of dolomite and calcite, which suggests cement growth through different diagenetic ''zones'' (e.g., Coleman 1995; Curtis et al. 1986). The presence of unlined vertical burrows in the top parts of many cement horizons, possibly indicating a firm substrate, may suggest possible early cementation in these bodies.

$\delta^{13}C$, $\delta^{18}O$, and $^{87}Sr/^{86}Sr$ Constraints.—$\delta^{13}C$ data (−3.8 to −6.8‰ VPDB) suggest that a significant component of carbonate was derived from organic-matter carbon. This is consistent with a cement origin during early diagenesis. However, $\delta^{18}O$ and $^{87}Sr/^{86}Sr$ data suggest precipitation from either meteoric fluids or during later burial diagenesis. Because of the small-scale zoning in these laterally extensive cement bodies, however, it was impossible to obtain single-phase cement data. The stable-isotope data must therefore be treated as a mixture of different cement components. The isotopic data suggest that in these laterally extensive cements the later burial cements are the most significant component, having isotopic compositions similar to that of the later cements in the concretionary cemented bodies (Figs 6, 7). Observations from the Book Cliffs (Taylor et al. 1995; unpublished data), however, show that these laterally extensive cemented zones become more significant in distal strata, and that in these distal locations cemented horizons are characterized by early, pore-occluding cements. Early diagenetic cementation has also been observed in laterally extensive cemented bodies in the Mancos Shale of the Book Cliffs area by Klein et al. (1999). These observations, together with the presence of zoned dolomite cements, suggest that some early cement precipitation took place in these cement zones.

On the basis of petrographic observations and the association of laterally extensive cements with marine flooding surfaces, we propose that cementation began at breaks in sediment accumulation during marine flooding events, at which time the rate of accommodation increase may outpace sediment supply, resulting in a significant reduction in sedimentation (Jervey 1988; Taylor et al. 1995). At low rates of sediment burial, sediment residence times in early diagenetic zones are high, thereby resulting in greater intensity of early diagenetic reactions (through replenishment of sulfate and methane through diffusion, and organic matter through bioturbation, and enhanced production of bicarbonate; Berner 1980; Curtis 1987). Consequently, low sediment accumulation rates may lead to enhanced localized cementation. Raiswell (1987) has similarly argued, from geochemical evidence, that such breaks in sediment accumulation lead to the formation of carbonate concretions in marine mudstone successions.

Following this initial cementation phase (Fig. 12B) carbonate cementation continued through later burial, nucleating on early carbonate cement. $\delta^{13}C$ data suggest that this later carbonate cement had a significant organic-matter source. The presence of organic-rich mudstones overlying the marine flooding surface would have resulted in a local source of bicarbonate through decarboxylation and iron reduction reactions taking place within the mudstones during sediment burial (Fig. 12C).

SUMMARY AND CONCLUSIONS

Three macroscopic diagenetic features can be recognized in the Upper Cretaceous strata of the Book Cliffs, each with distinctive form, geometry, and stratigraphic distribution. These diagenetic features are: (1) diagenetically leached zones (''whitecaps''); (2) large concretionary carbonate-cemented bodies; and (3) thin, laterally extensive carbonate-cemented horizons. These three features have distinct petrographic and geochemical signatures, and formed through discrete diagenetic processes (Fig. 12).

Large, isolated carbonate-cemented bodies in the Book Cliffs strata occupy a significant proportion of amalgamated sandstone bodies and would therefore significantly decrease reservoir quality in an analogous petroleum reservoir. These concretions occur in sandstone bodies downdip from coal beds, and cement precipitation resulted from meteoric remobilization of detrital dolomite from beneath coal beds during relative sea-level fall (Fig. 12A).

Laterally continuous cement bodies are present beneath major marine flooding surfaces. We propose that cement precipitation at these horizons began as a result of breaks in sediment accumulation during marine flooding events (relative sea-level rise). Cement precipitation continued during sediment burial as a result of organic-matter oxidation reactions in overlying organic-rich mudstones (Fig. 12B, C). Additional work is required on downdip to updip transects of these cemented horizons to delineate the relative control of each of these processes on the formation of these laterally continuous cement horizons.

The results of this study show a link between sedimentation (related to changes in relative sea level) and diagenesis. We believe that the integration of diagenetic analysis to large-scale, sequence stratigraphic studies provides the best mechanism for the construction of predictive models for early diagenesis in siliciclastic sedimentary successions.

ACKNOWLEDGMENTS

This work was funded by the Natural Environment Research Council (Grant No. GR3/8928 to RLG and CDC) and is gratefully acknowledged. Exxon Production Research Company, Houston, and, in particular, John Van Wagoner, are thanked for access to their stratigraphic data sets in the Book Cliffs. Morgan Sullivan, Mike Hayes, Joe Macquaker, Dave Hunt, and Fiona Burns are thanked for input and discussion throughout this study. JSR reviewers Penny Patterson and Bryan Bracken are thanked for their comments, which significantly improved the manuscript.

REFERENCES

Baldwin, B., and Butler, C.O., 1985, Compaction curves: American Association of Petroleum Geologists, Bulletin, v. 69, p. 622–626.

Berner, R.A., 1980, Early Diagenesis; A Theoretical Approach: Princeton, New Jersey, Princeton University Press, 241 p.

Bjørkum, P.A., and Walderhaug, A., 1990a, Geometrical arrangement of calcite cementation within shallow marine sandstones: Earth-Science Reviews, v. 29, p. 145–161.

Bjørkum, P.A., and Walderhaug, A., 1990b, Lateral extent of calcite cemented zones in shallow marine sandstones, *in* Buller, A.T., Berg, E., and Hjelmeland, E., eds., North Sea Oil and Gas Reservoirs II: London, Graham & Trotman, p. 331–336.

Burchfiel, B.C., Cowan, D.S., and Davis, G.A., 1992, Tectonic overview of the Cordilleran orogen in the western United States, *in* Burchfiel, B.C., Lipman, P.W., and Zoback, M.L., eds., The Cordilleran Orogen: Conterminous U.S.: Geological Survey of America, The Geology of North America, v. G-3, p. 407–480.

Burke, W.M., Denison, R.E., Hetherington, E.A., Koepnick, R.B., Nelson, M.F., and Otto, J.B., 1982, Variation in sea-water $^{87}Sr/^{86}Sr$ throughout Phanerozoic time: Geology, v. 10, p. 516–519.

Canfield, D.E., Raiswell, R., and Bottrell, S., 1992, The reactivity of sedimentary iron minerals towards sulfide: American Journal of Science, v. 292, p. 659–683.

Coleman, M.L., 1985, Geochemistry of diagenetic non-silicate minerals: kinetic considerations: Royal Society [London], Philosophical Transactions, v. A315, p. 39–56.

Coplen, T.B., 1994, Reporting of stable hydrogen, carbon and oxygen isotopic abundances, Technical report of the IUPAC inorganic chemistry division commission on atomic weights and isotopic abundances: Pure and Applied Chemistry, v. 66, p. 273–276.

Coplen, T.B., 1995, Reporting of stable carbon, hydrogen and oxygen isotopic abundances. In reference and intercomparison materials for stable isotopes of light elements, International Atomic Energy Authority, TECDOC 825, p. 31–34.

Craig, H., 1957, Isotopic standards for carbon and oxygen factors for mass-spectrometric analysis of carbon dioxide: Geochimica et Cosmochimica Acta, v. 12, p. 133–149.

Curtis, C.D., 1987, Inorganic chemistry and petroleum exploration, *in* Brooks, J., and Welte, D., eds., Advances in Petroleum Geochemistry II: London, Academic Press, p. 91–140.

Curtis, C.D., Coleman, M.L., and Love, L.G., 1986, Pore water evolution during sediment burial from isotope and mineral chemistry of calcite, dolomite and siderite concretions: Geochimica et Cosmochimica Acta, v. 50, p. 2321–2334.

Faure, G., Hurley, P.M., and Fairbairn, H.W., 1963, An estimation of strontium in rocks of the Precambrian Shield of North America: Journal of Geophysical Research, v. 68, p. 2323–2329.

Fouch, T.D., Lawton, T.F., Nichols, D.J., Cashion, W.B., and Cobban, W.A., 1983, Patterns and timing of synorogenic sedimentation in Upper Cretaceous rocks of Central and Northeast Utah, *in* Reynolds, M.W., and Dolly, E.D., eds., Mesozoic Paleogeography of the West Central United States: SEPM, Rocky Mountain Section, Rocky Mountain Paleogeography Symposium 2, p. 305–336.

Friedman, I., and O'Neil, J.R., 1977, Compilation of stable isotope fractionation factors of geochemical interest, *in* Fleischer, M., ed., Data of Geochemistry, 6th Edition: U.S. Geological Survey, Professional Paper 440-KK, vi + 12 p.

Hale, L.A., and Van De Graaff, F.R., 1964, Cretaceous stratigraphy and facies patterns—northeastern Utah and adjacent areas: Intermountain Association of Petroleum Geologists 13th Annual Field Conference, Guidebook to the Geology and Mineral Resources of the Uinta Basin—Utah's Hydrocarbon Storehouse, p. 115–138.

Hendry, J.P., Trewin, N.H., and Fallick, A.E., 1996, Low-Mg calcite cement in Cretaceous turbidites: origin, spatial distribution and relationship to seawater chemistry: Sedimentology, v. 43, p. 877–900.

Jervey, M.T., 1988, Quantitative geological modeling of siliciclastic rock sequences and their seismic expression, *in* Wilgus, C.K., Hastings, B.S., Kendall, C.G.St.C., Posamentier, H.W., Ross, C.A., and Van Wagoner, J.C., eds., Sea-Level Changes: An Integrated Approach: SEPM, Special Publication 42, p. 47–69.

Kantorowicz, J.D., Bryant, I.D., and Dawans, J.M., 1987, Controls on the geometry and distribution of carbonate cements in Jurassic sandstones: Bridport Sands, southern England and Viking Group, Troll Field, Norway, *in* Marshall, J.D., ed., Diagenesis of Sedimentary Sequences: Geological Society of London, Special Publication 36, p. 103–118.

Klein, J.S., Mozley, P., Campbell, A., and Cole, R., 1999, Spatial distribution of carbon and oxygen isotopes in laterally extensive carbonate cemented layers: implications for mode of growth and subsurface identification: Journal of Sedimentary Research, v. 69, p. 184–201.

Machemer, S.D., and Hutcheon, I., 1988, Geochemistry of early carbonate cements in the Cardium Formation, central Alberta: Journal of Sedimentary Petrology, v. 58, p. 136–147.

Manning, D.A.C., 1997, Acetate and propionate in landfill leachate: implications for recognition of microbiological influences on the composition of waters in sedimentary systems: Geology, v. 25, p. 279–281.

Manning, D.A.C., and Bewsher, A., 1997, Determination of anions in landfill leachates by ion chromatography: Journal of Chromatography A, v. 770, p. 203–210.

Manning, D.A.C., Gestsdottir, K., and Rae, E.I.C., 1992, Feldspar dissolution in the presence of organic-acid anions under diagenetic conditions—an experimental study: Organic Geochemistry, v. 19, p. 483–492.

Manning, D.A.C., Rae, E.I.C., and Gestsdottir, K., 1994, Appraisal of the use of experimental and analogue studies in the assessment of the role of organic-acid anions in diagenesis: Marine and Petroleum Geology, v. 11, p. 10–19.

Matthews, A., and Katz, A., 1977, Oxygen isotope fractionation during the dolomitisation of calcium carbonate: Geochimica et Cosmochimica Acta, v. 41, p. 1431–1438.

McBride, E.F., Picard, M.D., and Folk, R.L., 1994, Oriented concretions, Ionian Coast, Italy: Journal of Sedimentary Research, v. A64, p. 535–540.

McBride, E.F., Milliken, K.L., Cavazza, W., Cibin, U., Fontana, D., Picard, D., and Zuffa, G., 1995, Heterogeneous distribution of calcite cement at the outcrop scale in Tertiary sandstones, northern Appennines, Italy: American Association of Petroleum Geologists, Bulletin, v. 79, p. 1044–1063.

McKay, J.L., Longstaffe, F.J., and Plint, A.G., 1995, Early diagenesis and its relationship to depositional environment and relative sea-level fluctuations (Upper Cretaceous Marshybank Formation, Alberta and British Columbia): Sedimentology, v. 42, p. 161–190.

Mozley, P.S., and Davis, J.M., 1996, Relationship between oriented calcite concretions and permeability correlation structure in an alluvial aquifer, Sierra Ladrones Formation, New Mexico: Journal of Sedimentary Research, v. A66, p. 11–16.

O'Byrne, C.J., and Flint, S., 1995, Sequence, parasequence, and intraparasequence architecture of the Grassy Member, Blackhawk Formation, Book Cliffs, Utah, U.S.A., *in* Van Wagoner, J.C. and Bertram, G.T., eds., Sequence Stratigraphy of Foreland Basin Deposits: American Association of Petroleum Geologists, Memoir 64, p. 225–255.

Percival, C.J., 1983, The Firestone Sill ganister, Namurian, Northern England—the A2 horizon of a podzol or podzolic palaeosol: Sedimentary Geology, v. 36, p. 41–49.

Postma, D., 1993, The reactivity of iron oxides in sediments: a kinetic approach: Geochimica et Cosmochimica Acta, v. 57, p. 5027–5034.

Prosser, D.J., Daws, J.A., Fallick, A.E., and Williams, B.P.J., 1993, Geochemistry and diagenesis of stratabound calcite cement layers within the Rannoch Formation of the Brent Group, Murchison Field, North Viking Graben (Northern North Sea): Sedimentary Geology, v. 87, p. 139–164.

Raiswell, R., 1987, Non-steady state microbiological diagenesis and the origin of concretions and nodular limestones, *in* Marshall, J.D., ed., Diagenesis of Sedimentary Sequences: Geological Society of London, Special Publication 36, p. 41–54.

Shackleton, N.J., and Kennett, J.P., 1975, Late Cenozoic oxygen and carbon isotopic change at DSDP site 284: implications for the glacial history of the Northern Hemisphere, *in* Kennett, J.P., et al., eds., Initial Reports of the Deep Sea Drilling Project, v. 29, p. 801–807.

Surdam, R.C., Crossey, L.J., Hagen, E.S., and Heasler, H.P., 1989, Organic–inorganic interactions and sandstone diagenesis: American Association of Petroleum Geologists, Bulletin, v. 73, p. 1–23.

TAYLOR, K.G., GAWTHORPE, R.L., AND VAN WAGONER, J.C., 1995, Stratigraphic control on laterally persistent cementation, Book Cliffs, Utah: Geological Society of London, Journal, v. 152, p. 225–228.

TUCKER, M.E., AND WRIGHT, V.P., 1990, Carbonate Sedimentology: Oxford, U.K., Blackwell, 482 p.

VAN DE GRAAFF, F.R., 1969, Depositional environments and petrology of the Castlegate sandstone (Cretaceous), east-central Utah [unpublished Ph.D. thesis]: University of Missouri, Columbia, Missouri, 120 p.

VAN DE GRAAFF, F.R., 1972, Fluvial–deltaic facies of the Castlegate Sandstone (Cretaceous), east-central Utah: Journal of Sedimentary Petrology, v. 42, p. 558–571.

VAN KEER, I., MUCHEZ, P., AND VIAENE, W., 1998, Clay mineralogical variations and evolutions in sandstone sequences near a coal seam and shales in the Westphalian of the Campine Basin (NE Belgium): Clay Minerals, v. 33, p. 159–169.

VAN WAGONER, J.C., 1991, Sequence stratigraphy and facies architecture of the Desert Member of the Blackhawk Formation and the Castlegate Formation in the Book Cliffs of eastern Utah and western Colorado, *in* Van Wagoner, J.C., Jones, C.R., Taylor, D.R., Nummedal, D., Jennette, D.C., and Riley, G.W., eds., Sequence Stratigraphy Applications to Shelf Sandstone Reservoirs: Outcrop to Subsurface Examples. American Association of Petroleum Geologists Field Conference, September 1991, 12 p.

VAN WAGONER, J.C., 1995, Sequence stratigraphy and marine to non-marine facies architecture of foreland basin strata, Book Cliffs, Utah, U.S.A., *in* Van Wagoner, J.C., and Bertram, G.T., eds., Sequence Stratigraphy of Foreland Basin Deposits: American Association of Petroleum Geologists, Memoir 64, p. 137–223.

VAN WAGONER, J.C., MITCHUM, R.M., CAMPION, K.M., AND RAHMANIAN, V.D., 1990, Siliciclastic sequence stratigraphy in well logs, cores, and outcrops: concepts for high resolution correlation of time and facies: American Association of Petroleum Geologists, Methods in Exploration Series 7, 55 p.

WILKINSON, M., 1991, The concretions of the Bearreraig Sandstone Formation: geometry and geochemistry: Sedimentology, v. 38, p. 899–912.

Received 23 July 1998; accepted 28 July 1999.